

Electronic Supplementary Information for

**Light-induced confinement of electrons in stacked distorted graphene layers  
– (TD-)DFT study**

Adam Olejniczak<sup>1\*</sup>, Bartłomiej Cichy<sup>1\*</sup>, Lukasz Radosinski<sup>2</sup>, Wieslaw Strek<sup>1</sup>

<sup>1</sup>*Department of Spectroscopy of Excited States, Institute of Low Temperature and Structure Research, Polish Academy of Sciences, Okólna 2, Wrocław, 50-422, Poland*

<sup>2</sup>*Wroclaw University of Technology, Chemistry Department, Group of Bioprocess and Biomedical Engineering, Wybrzeze Wyspianskiego 27, 50-370 Wroclaw, Poland*

\*corresponding authors: b.cichy@int.pan.wroc.pl, a.olejniczak@int.pan.wroc.pl

Following figures (Fig. S1-S9) present structures of HHC clusters considered in this work after geometry optimization in ground ( $S_0$ ) state. Brown spheres indicate carbon atoms and white spheres indicate hydrogen atoms. Top view (up) and side view (down) of HHC clusters are presented on every S1-S9 figures.

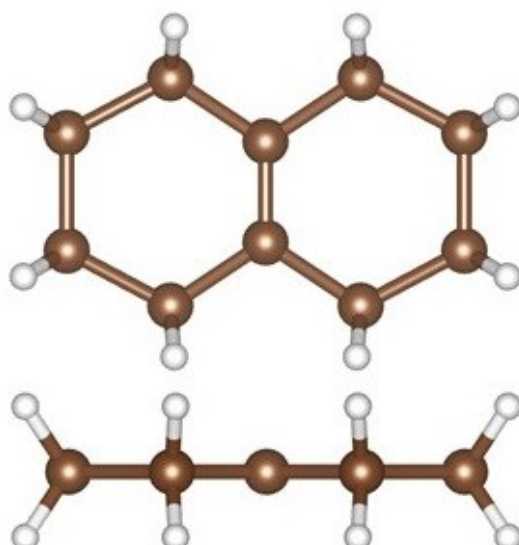


Figure S1. Top view (up) and side view (down) of HHC10 graphene cluster.

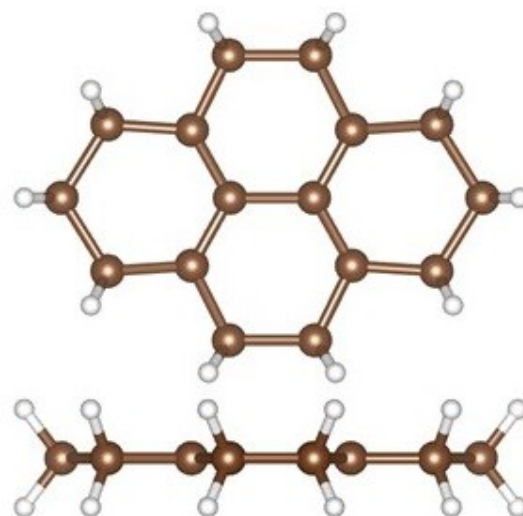


Figure S2. Top view (up) and side view (down) of HHC16 graphene cluster.

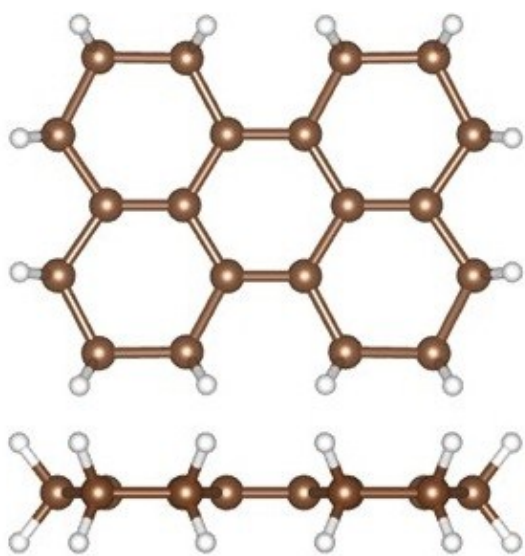


Figure S3. Top view (up) and side view (down) of HHC20 graphene cluster.

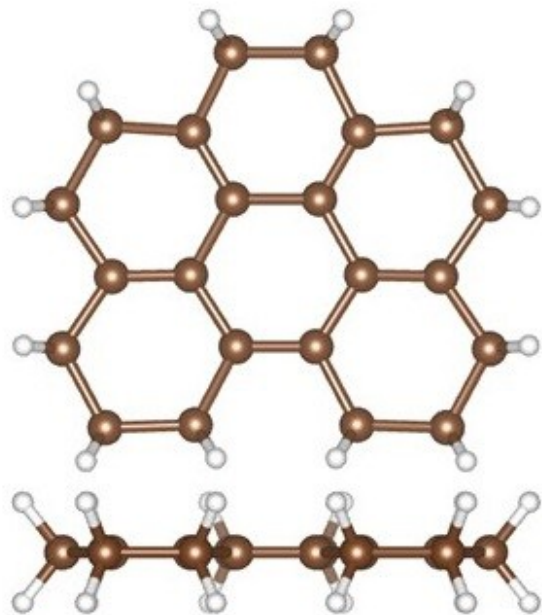


Figure S4. Top view (up) and side view (down) of HHC22 graphene cluster.

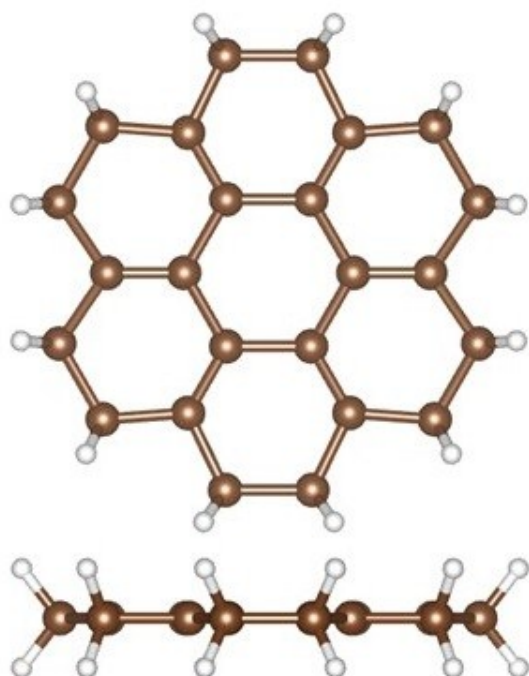


Figure S5. Top view (up) and side view (down) of HHC24 graphene cluster.

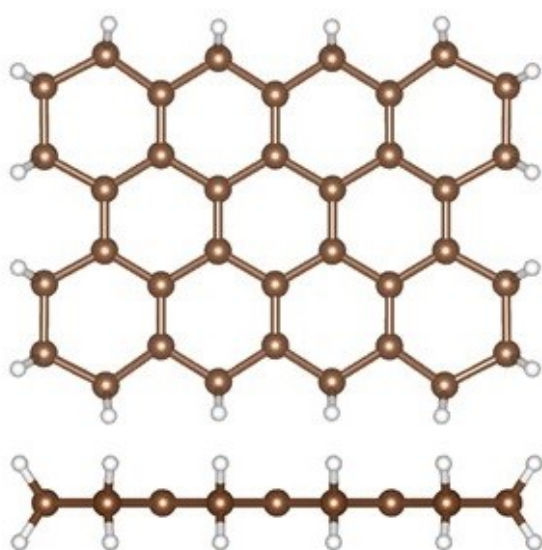


Figure S4. Top view (up) and side view (down) of HHC36 graphene cluster.

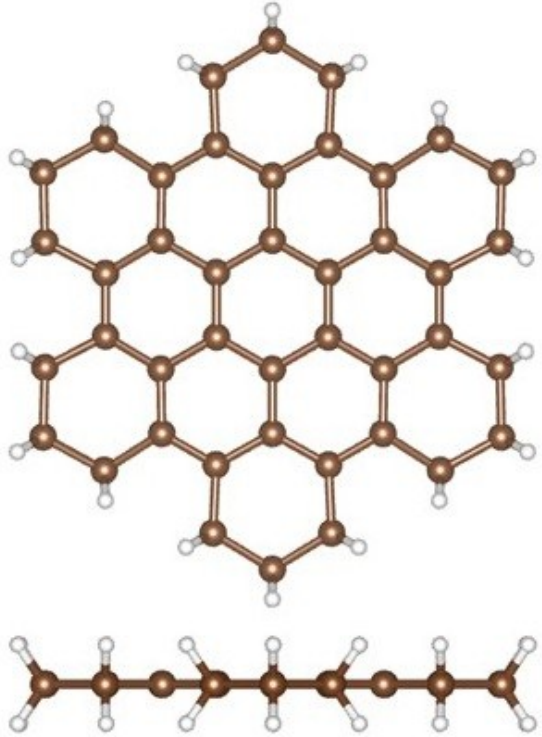


Figure S5. Top view (up) and side view (down) of HHC42 graphene cluster.

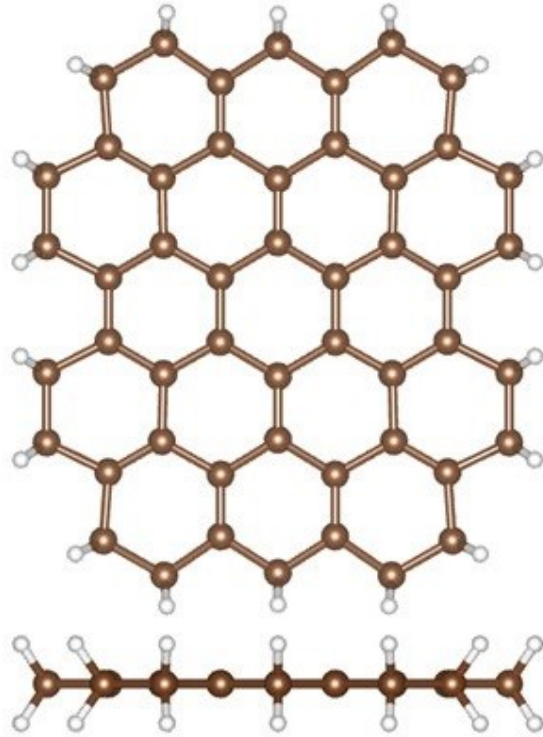


Figure S8. Top view (up) and side view (down) of HHC50 graphene cluster.

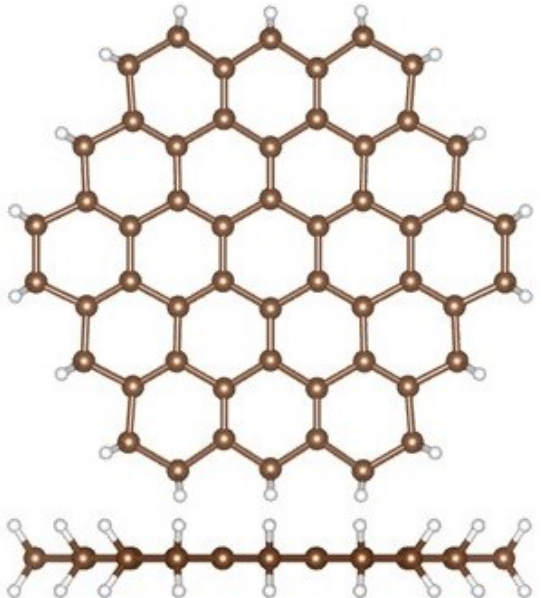


Figure S9. Top view (up) and side view (down) of HHC54 graphene cluster.

Table S1. The values of energy gaps (in eV) between allowed electrons energy level in  $\pi$ - $\pi^*$  area with corresponding wavelengths (in nm). Symbol Ln (Hn) denotes n-th level above (below) LUMO (HOMO) level. HOMO-LUMO energy gap is denoted as H-L. Wavelengths belonging to VIS spectrum was colored with corresponding color, and those belonging to NIR spectrum was colored in brown.

Table S2. Vertical excitation energies (in eV) for the first 20 singlets together with corresponding oscillator strengths for every structure. Excitation with oscillator strengths values greater than 0.01 are given bold.

| Transition          | HHC10                        | HHC16                        | HHC20                        | HHC22                        | HHC24                        | HHC36                        | HHC42                        | HHC50                        | HHC54                        |
|---------------------|------------------------------|------------------------------|------------------------------|------------------------------|------------------------------|------------------------------|------------------------------|------------------------------|------------------------------|
| S0-S1<br>osc. str.  | <b>6.94</b><br><b>0.0182</b> | <b>1.59</b><br><b>0.1187</b> | <b>3.72</b><br><b>0.8147</b> | 3.13                         | 2.44                         | 2.50                         | 3.02                         | 1.93                         | 1.02                         |
| S0-S2<br>osc. str.  | <b>6.98</b><br><b>0.4308</b> | 3.01                         | 4.08                         | <b>3.43</b><br><b>0.0205</b> | 3.30                         | <b>2.60</b><br><b>0.0726</b> | 3.23                         | 2.09                         | 1.53                         |
| S0-S3<br>osc. str.  | 7.53<br>0.0000               | <b>4.47</b><br><b>0.6991</b> | 4.30                         | <b>3.56</b><br><b>0.0480</b> | 3.30                         | 2.81                         | <b>3.84</b><br><b>0.8432</b> | <b>2.17</b><br><b>0.2782</b> | 1.53<br>0.0000               |
| S0-S4<br>osc. str.  | 7.65<br>0.0000               | 4.61<br>0.0                  | 5.30<br>0.0000               | <b>3.91</b><br><b>0.6437</b> | 3.68<br>0.0000               | 3.05<br>0.0000               | <b>3.84</b><br><b>0.8433</b> | <b>2.32</b><br><b>0.3946</b> | 1.72<br>0.0000               |
| S0-S5<br>osc. str.  | 7.68<br>0.0000               | 4.66<br>0.0000               | 5.46<br>0.0000               | 5.39<br>0.0009               | 3.68<br>0.0000               | <b>3.70</b><br><b>0.1497</b> | 4.08<br>0.0000               | 2.35<br>0.0039               | 1.72<br>0.0000               |
| S0-S6<br>osc. str.  | <b>7.78</b><br><b>0.0392</b> | 4.99                         | 5.78                         | <b>5.41</b><br><b>0.0318</b> | 4.28                         | 3.37                         | 4.08                         | <b>2.52</b><br><b>0.0539</b> | 2.04<br>0.0000               |
| S0-S7<br>osc. str.  | 7.85<br>0.0000               | <b>5.07</b><br><b>0.0231</b> | 5.88<br>0.0000               | 5.70<br>0.0008               | <b>4.61</b><br><b>0.3364</b> | <b>3.45</b><br><b>0.3070</b> | 4.11<br>0.0000               | 2.64<br>0.0000               | 2.25<br>0.0000               |
| S0-S8<br>osc. str.  | 8.25<br>0.0000               | <b>5.26</b><br><b>0.0101</b> | 5.90<br>0.0000               | 5.82<br>0.0002               | <b>4.61</b><br><b>0.3364</b> | 3.78<br>0.0000               | 4.18<br>0.0000               | 2.85<br>0.0000               | <b>2.32</b><br><b>0.4495</b> |
| S0-S9<br>osc. str.  | <b>8.39</b><br><b>0.0279</b> | 5.38                         | 5.97                         | 5.85<br>0.0009               | 4.63<br>0.0000               | 4.03<br>0.0000               | 4.31<br>0.0000               | 2.91<br>0.0000               | <b>2.32</b><br><b>0.4495</b> |
| S0-S10<br>osc. str. | <b>8.75</b><br><b>0.0123</b> | 5.54                         | <b>6.20</b><br><b>0.5795</b> | 5.86<br>0.0000               | 5.51<br>0.0000               | 4.23<br>0.0000               | 4.40<br>0.0000               | 3.09<br>0.0000               | 2.34<br>0.0000               |
| S0-S11<br>osc. str. | 8.82<br>0.0000               | 5.78                         | 6.32                         | <b>5.92</b><br><b>0.2996</b> | 5.51<br>0.0000               | <b>4.25</b><br><b>0.0198</b> | 4.40<br>0.0000               | 3.12<br>0.0026               | 2.51<br>0.0001               |
| S0-S12<br>osc. str. | 8.89<br>0.0000               | <b>5.79</b><br><b>0.0108</b> | 6.37                         | 5.93<br>0.0000               | 5.54<br>0.0000               | 4.38<br>0.0000               | 4.71<br>0.0000               | <b>3.29</b><br><b>0.0166</b> | 2.51<br>0.0001               |
| S0-S13<br>osc. str. | 9.03<br>0.0000               | 5.89                         | 6.50                         | <b>5.94</b><br><b>0.0744</b> | <b>5.74</b><br><b>0.1006</b> | <b>4.51</b><br><b>0.3720</b> | 4.73<br>0.0000               | <b>3.30</b><br><b>0.1609</b> | 2.60<br>0.0000               |
| S0-S14<br>osc. str. | 9.09<br>0.0000               | <b>5.90</b><br><b>0.3776</b> | 6.54                         | <b>5.95</b><br><b>0.0785</b> | <b>5.74</b><br><b>0.1007</b> | 4.62<br>0.0079               | 4.73<br>0.0000               | <b>3.53</b><br><b>0.0248</b> | 2.81<br>0.0034               |
| S0-S15<br>osc. str. | 9.16<br>0.0000               | 5.91                         | 6.56                         | 6.07<br>0.0097               | 5.81<br>0.0000               | 4.73<br>0.0000               | 4.85<br>0.0000               | 3.62<br>0.0000               | 2.81<br>0.0034               |
| S0-S16<br>osc. str. | 9.33<br>0.0000               | 6.07                         | <b>6.64</b><br><b>0.0149</b> | 6.19<br>0.0000               | 5.81<br>0.0000               | <b>4.74</b><br><b>1.1515</b> | 4.85<br>0.0000               | 3.70<br>0.0000               | 3.07<br>0.0004               |
| S0-S17<br>osc. str. | 9.38<br>0.0000               | <b>6.12</b><br><b>0.2322</b> | 6.70                         | 6.20<br>0.0022               | 5.96<br>0.0000               | 4.99<br>0.0000               | 5.10<br>0.0000               | 3.74<br>0.0000               | 3.07<br>0.0004               |
| S0-S18<br>osc. str. | <b>9.39</b><br><b>0.0103</b> | 6.34                         | 6.76                         | 6.24<br>0.0020               | <b>6.33</b><br><b>0.4803</b> | 5.02<br>0.0000               | 5.10<br>0.0000               | 3.75<br>0.0000               | 3.17<br>0.0000               |
| S0-S19<br>osc. str. | 9.43<br>0.0000               | <b>6.42</b><br><b>0.0285</b> | <b>6.83</b><br><b>0.0360</b> | 6.27<br>0.0000               | <b>6.33</b><br><b>0.4803</b> | <b>5.06</b><br><b>0.0985</b> | 5.20<br>0.0000               | <b>3.77</b><br><b>0.1304</b> | 3.17<br>0.0000               |
| S0-S20<br>osc. str. | 9.56<br>0.0000               | 6.44                         | 6.87                         | <b>6.31</b><br><b>0.3378</b> | 6.38<br>0.0000               | 5.14<br>0.0000               | 5.48<br>0.0000               | 3.79<br>0.0005               | <b>3.18</b><br><b>0.0135</b> |

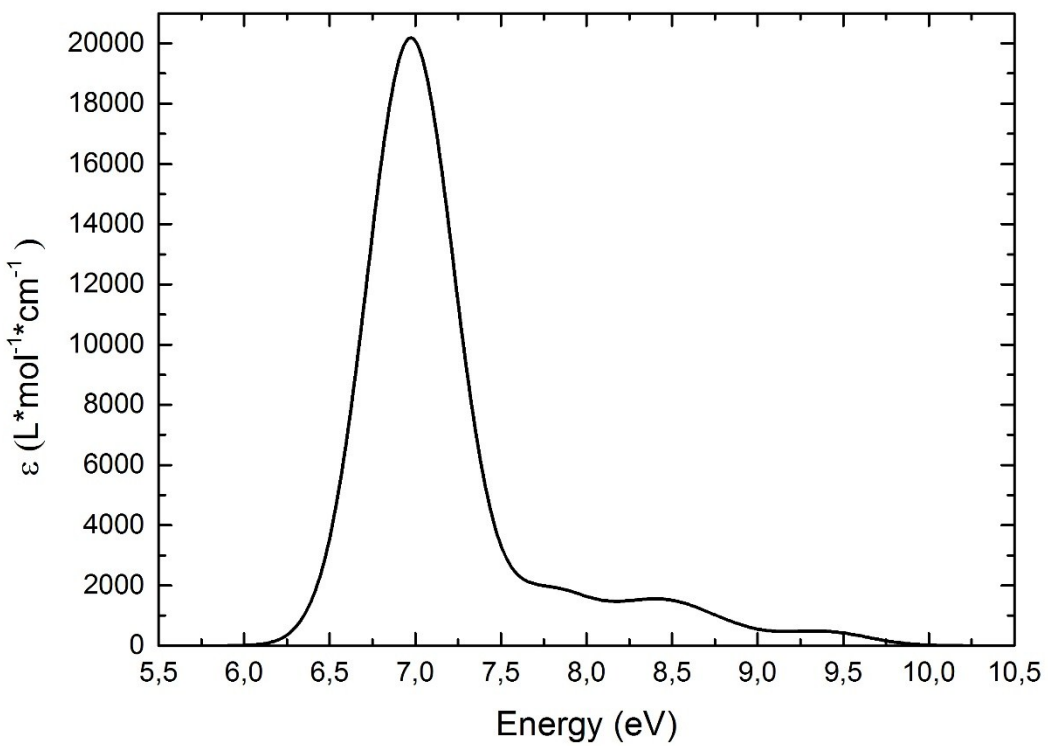


Figure S10. Absorption spectrum of HHC10 cluster.

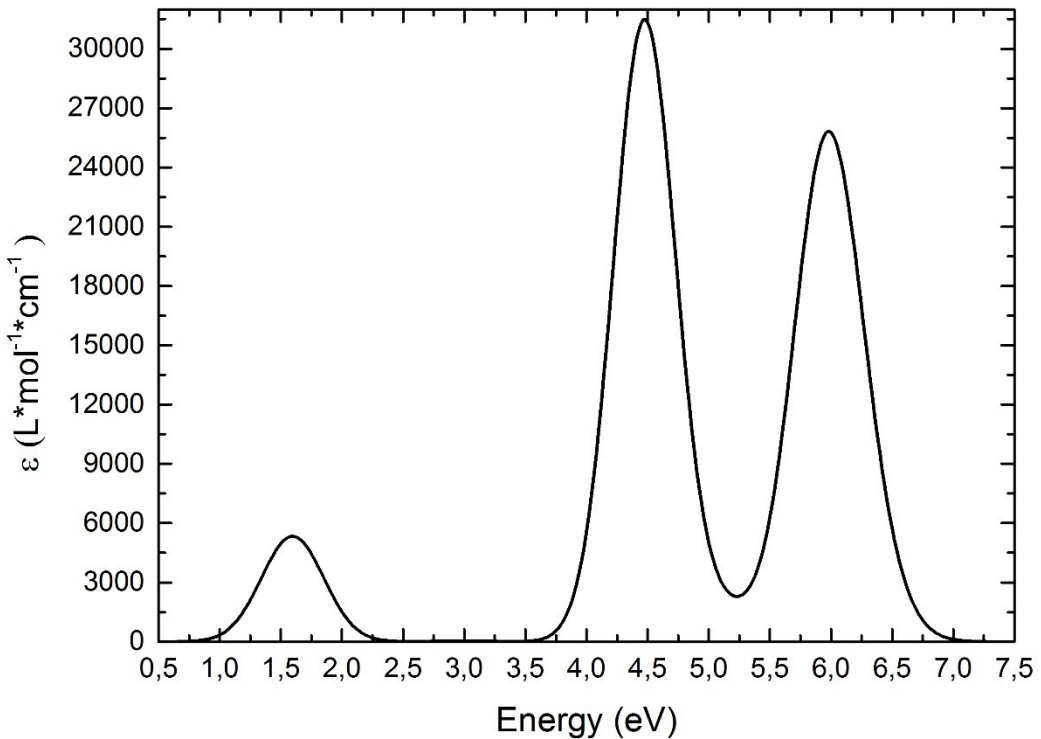


Figure S11. Absorption spectrum of HHC16 cluster.

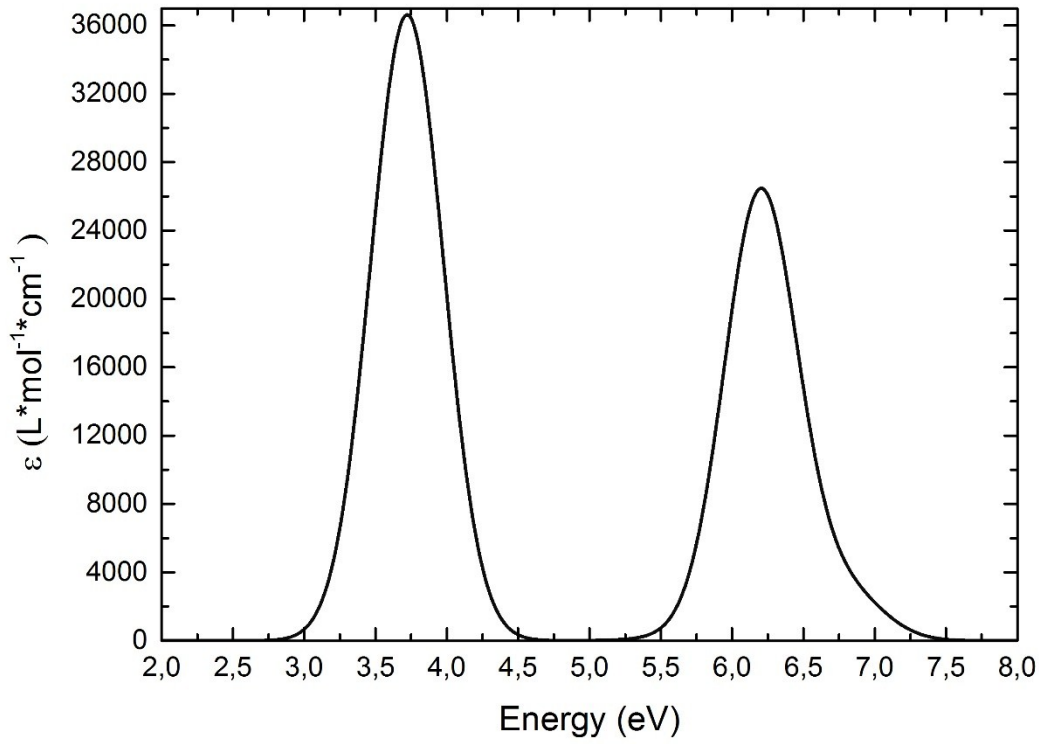


Figure S12. Absorption spectrum of HHC20 cluster.

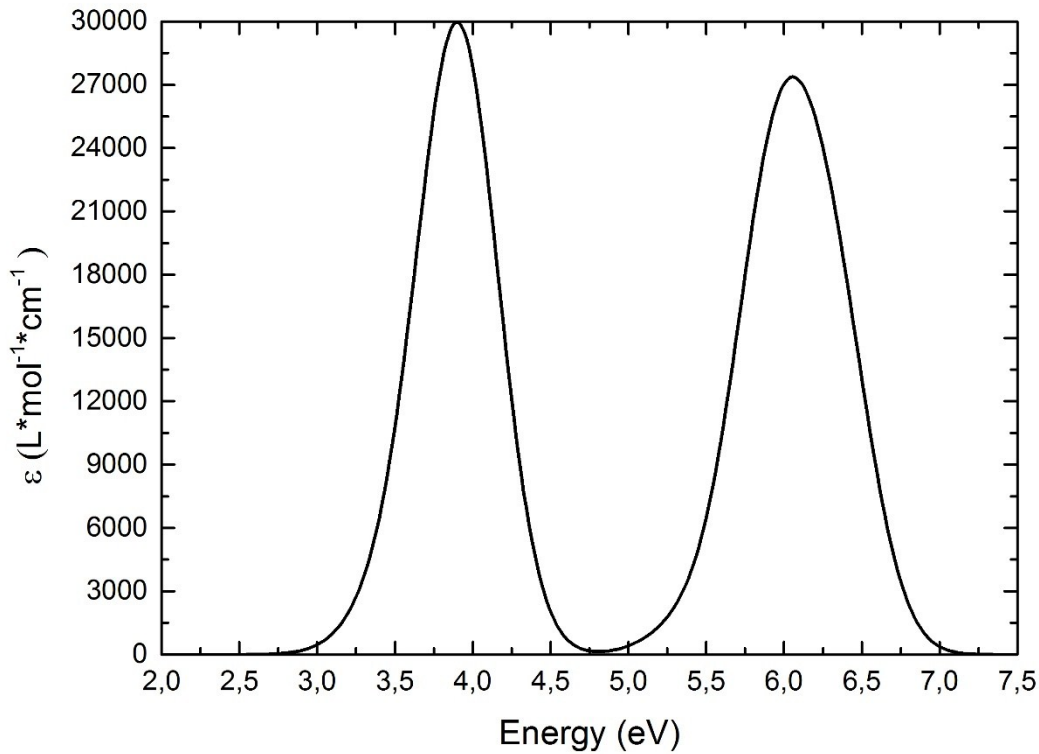


Figure S13. Absorption spectrum of HHC22 cluster.

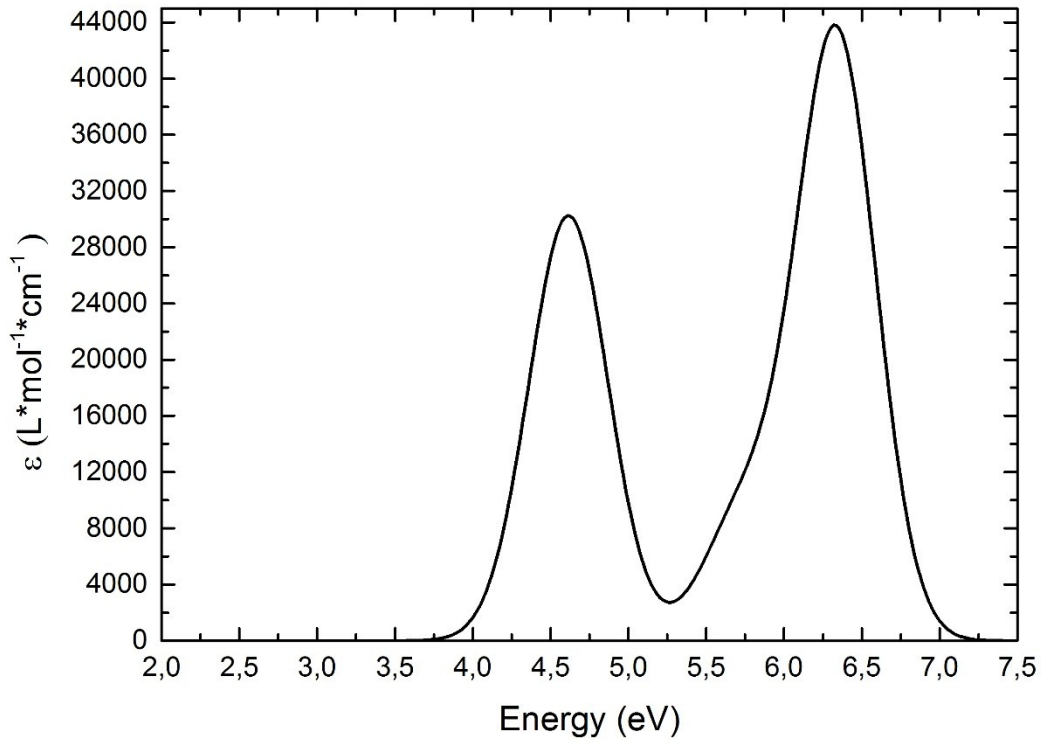


Figure S14. Absorption spectrum of HHC24 cluster.

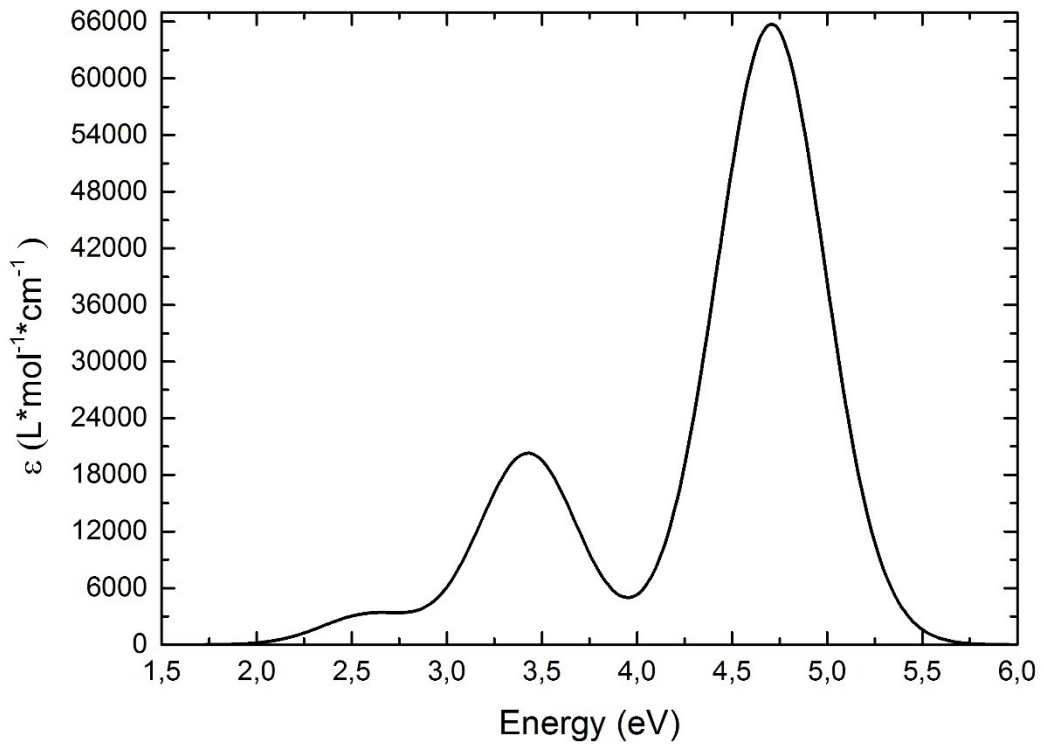


Figure S15. Absorption spectrum of HHC36 cluster.

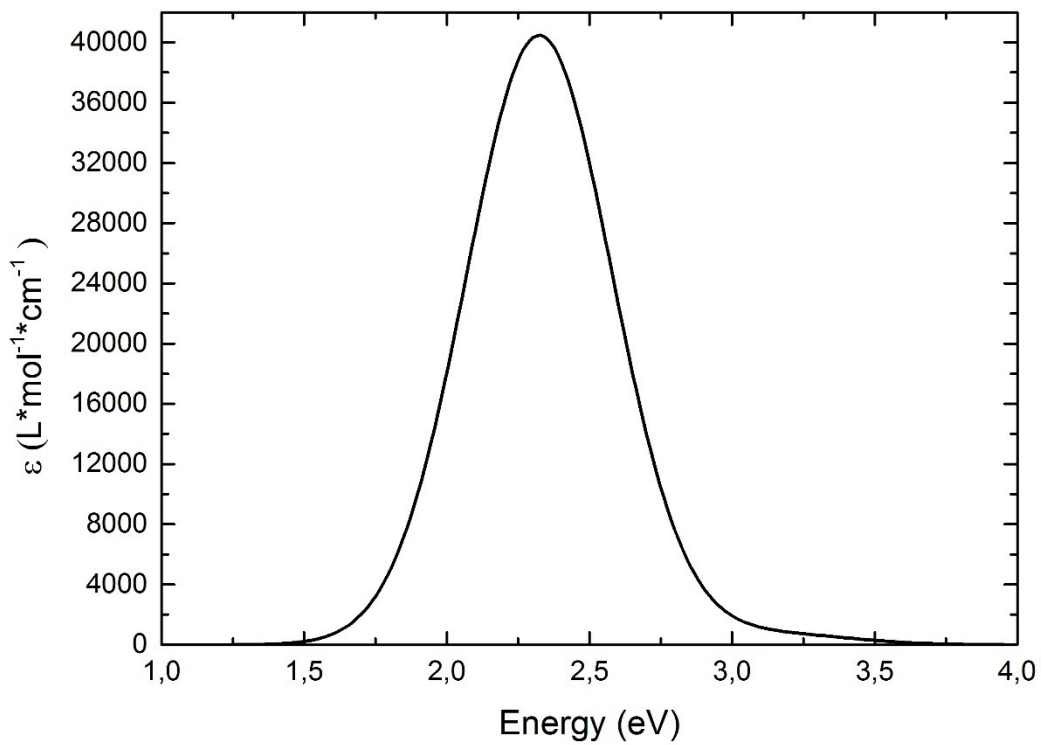


Figure S16. Absorption spectrum of HHC42 cluster.

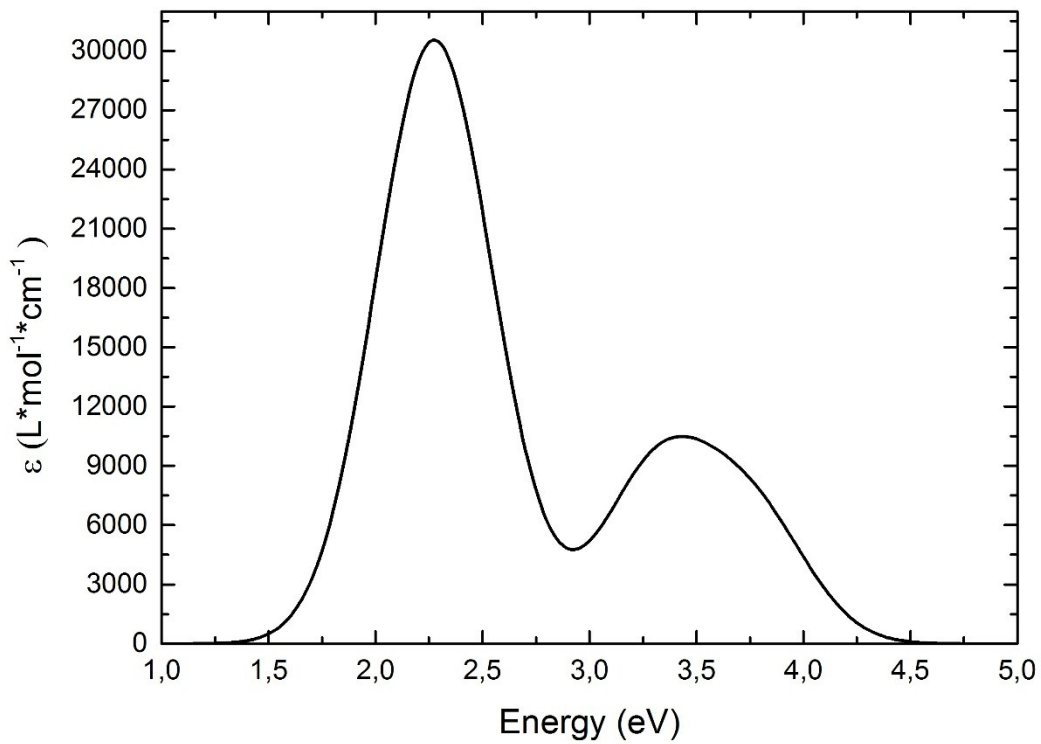


Figure S17. Absorption spectrum of HHC50 cluster.

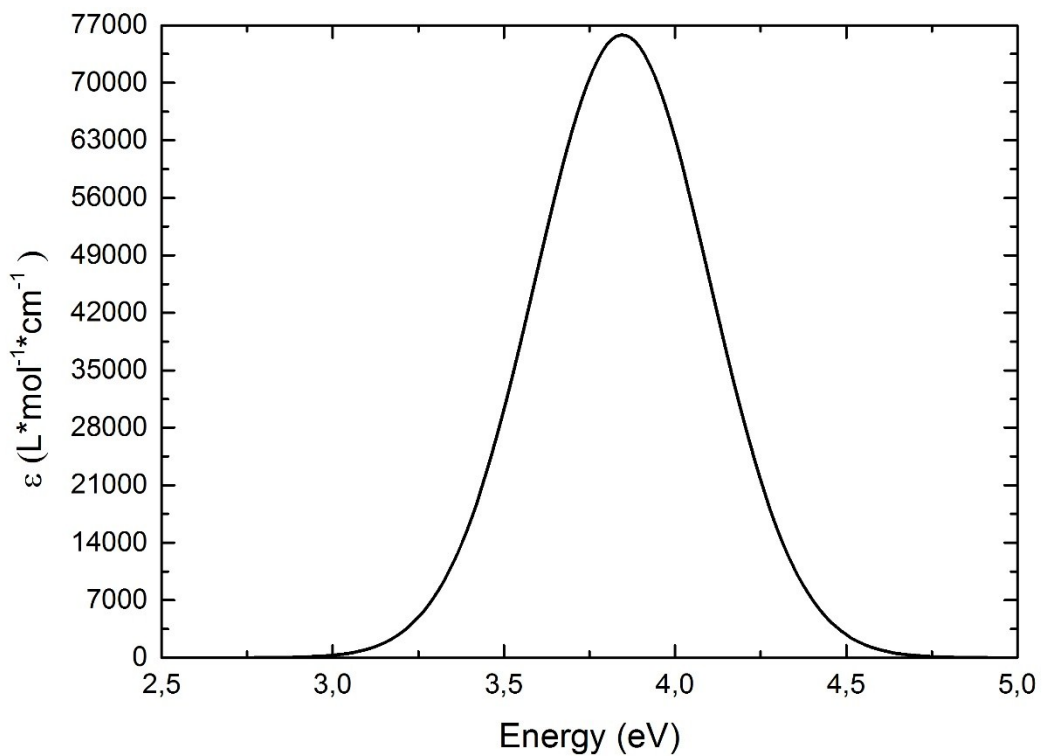


Figure S18. Absorption spectrum of HHC54 cluster.